Article

c-Met-Dependent Multipotent Labyrinth Trophoblast Progenitors Establish Placental Exchange Interface

Masaya Ueno,[1] Lydia K. Lee,[1] Akanksha Chhabra,[1] Yeon Joo Kim,[1] Rajkumar Sasidharan,[1] Ben Van Handel,[1] Ying Wang,[5] Masakazu Kamata,[6] Paniz Kamran,[3,7] Konstantina-Ioanna Sereti,[3,7] Reza Ardehali,[3,7] Meisheng Jiang,[5] and Hanna K.A. Mikkola[1,2,3,4,*]

[1]Department of Molecular, Cell and Developmental Biology
[2]Department of Microbiology, Immunology and Molecular Genetics
[3]Eli and Edythe Broad Center for Regenerative Medicine and Stem Cell Research
[4]Jonsson Comprehensive Cancer Center
[5]Molecular and Medical Pharmacology, School of Medicine
[6]Department of Hematology and Oncology
[7]Department of Cardiology, David Geffen School of Medicine
University of California, Los Angeles, Los Angeles, CA 90095, USA
*Correspondence: hmikkola@mcdb.ucla.edu
http://dx.doi.org/10.1016/j.devcel.2013.10.019

SUMMARY

The placenta provides the interface for gas and nutrient exchange between the mother and the fetus. Despite its critical function in sustaining pregnancy, the stem/progenitor cell hierarchy and molecular mechanisms responsible for the development of the placental exchange interface are poorly understood. We identified an Epcam[hi] labyrinth trophoblast progenitor (LaTP) in mouse placenta that at a clonal level generates all labyrinth trophoblast subtypes, syncytiotrophoblasts I and II, and sinusoidal trophoblast giant cells. Moreover, we discovered that hepatocyte growth factor/c-Met signaling is required for sustaining proliferation of LaTP during midgestation. Loss of trophoblast c-Met also disrupted terminal differentiation and polarization of syncytiotrophoblasts, leading to intrauterine fetal growth restriction, fetal liver hypocellularity, and demise. Identification of this c-Met-dependent multipotent LaTP provides a landmark in the poorly defined placental stem/progenitor cell hierarchy and may help us understand pregnancy complications caused by a defective placental exchange.

INTRODUCTION

The mammalian placenta serves as the interface for gas and nutrient exchange during development. The placenta also provides an immunological barrier between the fetus and the mother and secretes hormones that regulate pregnancy. Recent studies identified the placenta as a hematopoietic organ that generates hematopoietic stem/progenitor cells (HS/PC) and macrophages and provides a niche that protects definitive HS/PC from premature erythroid differentiation (Gekas et al.,

2005; Rhodes et al., 2008; Van Handel et al., 2010; Chhabra et al., 2012). Dysfunctional placental development has been associated with maternal hypertension and preeclampsia (Young et al., 2010), while disruption of placental circulation and fetal-maternal exchange can lead to intrauterine fetal growth restriction (IUGR) and demise (Scifres and Nelson, 2009). Therefore, proper placental function is critical for a healthy pregnancy.

In the mouse placenta, substance exchange occurs in the labyrinth (La; analogous to chorionic villi in human), which is composed of highly branched fetal vasculature and trophoblast-lined maternal blood spaces (Figure S1A available online; Rossant and Cross, 2001; Watson and Cross, 2005; Maltepe et al., 2010). Trophoblasts are epithelial cells that develop from the trophectoderm (Te), the outermost layer of the blastocyst. Mitotic activity is limited to polar Te that differentiates into chorionic trophoblasts and the ectoplacental cone (EPC). Chorionic trophoblasts form the labyrinth, while the EPC gives rise to the junctional zone (JZ) consisting of spongiotrophoblasts (Sp) and trophoblast giant cells (TGC) that provide structural support and enable invasion to the uterus (Figure 1A; Figure S1A). Morphogenesis of the labyrinth occurs after fusion of the allantoic mesoderm with chorionic trophoblasts (embryonic day 8.5 [E8.5]), which undergo extensive branching (Figure 1A). The labyrinth consists of two layers of multinucleated syncytiotrophoblasts (SynT-I and -II) that control fetal-maternal transport, and sinusoidal trophoblast giant cells (sTGCs) that have endocrine functions and act as hematopoietic signaling centers (Chhabra et al., 2012). Fibroblast growth factor 4 (Fgf4)-dependent trophoblast stem (TS) cells that generate all trophoblast subtypes can be established from the blastocyst and early postimplantation embryos, and are the in vitro equivalents of Te (Tanaka et al., 1998). However, TS cell potential disappears after chorioallantoic fusion (Uy et al., 2002) suggesting that yet unidentified precursors downstream of TS cells form the placenta (Figure 1A; Simmons and Cross, 2005). Recent studies identified an EPC-derived Blimp1^{+} precursor that generates multiple types of TGC in the Sp layer (Mould et al., 2012). However, the precursors

that generate the exchange interface in the placental labyrinth are unknown.

Targeted mutagenesis in mice has provided clues to mechanisms regulating key stages of placental development (Rossant and Cross, 2001; Watson and Cross, 2005). c-Met receptor tyrosine kinase and its ligand, hepatocyte growth factor (Hgf), have been identified as regulators of labyrinth morphogenesis. *Hgf* and *c-Met* knockout (KO) embryos exhibit IUGR and a smaller placenta and die by E14.5; Bladt et al., 1995; Schmidt et al., 1995; Uehara et al., 1995). c-Met signaling governs various morphogenetic events in development, tissue repair, and cancer metastasis by regulating cell growth and motility and stem/progenitor cells in multiple tissues express c-Met (Boccaccio and Comoglio, 2006). Nevertheless, little is known about the cellular and molecular mechanisms of how c-Met signaling governs placental development, and the extent to which placental dysfunction underlies the defective development of c-Met-deficient embryos.

Here we identify an Hgf/c-Met signaling-dependent Epcam[hi] multipotent labyrinth progenitor that gives rise to all labyrinth trophoblast subtypes. Trophoblast-specific loss of *c-Met* abrogated the proliferation of labyrinth trophoblast progenitors (LaTPs) and terminal differentiation and polarization of syncytiotrophoblasts, compromising both placental and fetal development. These discoveries advance our understanding of placental stem/progenitor cell hierarchy and provide an in vivo model for studying how dysfunctional placental exchange compromises pregnancy.

RESULTS

Epcam Marks Proliferative, Undifferentiated Trophoblasts in the Placental Labyrinth

To identify candidate trophoblast progenitor cells in the placental labyrinth, proliferative cells were labeled with bromodeoxyuridine (BrdU) 1 hr before dissection, and immunofluorescence (IF) was performed for BrdU and CD9 or Epcam (Trop1; Figure 1B; Figure S1A). CD9, a trophoblast marker upregulated at E10.5 during labyrinth morphogenesis (Wynne et al., 2006), was expressed broadly in syncytiotrophoblasts (SynT) in E12.5 labyrinth (Figure 1B; Figure S1A). In contrast, Epcam, a marker of many epithelial stem cells (McQualter et al., 2010), was expressed highly in a subset of labyrinth trophoblasts, while SynT showed low expression (Figure 1B; Figure S1A). Moreover, Epcam^{hi} cells were arranged in clusters and showed much higher frequency of BrdU incorporation than CD9^{+} cells (Figure 1B). To assess whether Epcam^{hi} cells are undifferentiated trophoblasts, sections were costained for monocarboxylate transporter (Mct) 4, which is expressed in the basal plasma membrane of SynT-II (Nagai et al., 2010) adjacent to fetal vasculature. Mct4 was undetectable by IF at E10.5 (data not shown), whereas by E12.5, Mct4 colocalized with Epcam in SynT-II (Epcam[low]; Figure 1C). In contrast, Epcam^{hi} cells were devoid of Mct4 expression (Figure 1C). At E9.5, Epcam^{hi} cells resided at the site of chorioallantoic fusion (Figure 1D), and by E12.5, they formed clusters adjacent to laminin^{+} stromal cells in the labyrinth. No Epcam^{hi} cells were detectable after completion of labyrinth morphogenesis at E14.5 (Figure 1D). These data nominated Epcam^{hi} cells as candidate progenitor cells in the placental labyrinth.

To define the identity of Epcam^{hi} cells, magnetic bead selection was used to isolate them from E10.5 placenta (Figure 1E; Figure S1B). Fluorescence-activated cell sorting (FACS) analysis confirmed the enrichment of Epcam^{hi} cells without a significant contribution of Epcam^{low} CD9^{hi} SynT (Figure S1B). Results of quantitative RT-PCR (qRT-PCR) indicated that the expression of genes required for labyrinth trophoblast development, including transcription factors *Gcm1*, *Dlx3*, and *Ovol2* (Morasso et al., 1999; Anson-Cartwright et al., 2000; Unezaki et al., 2007), and orphan nuclear factor *Nr6a1* (Morasso et al., 1999), was enriched in Epcam[hi] fraction in E10.5 placenta as compared to Epcam^{−} cells or TS cells (Figure 1F). Low expression of sTGC markers (*Ctsq* and *Prl3b*) was detected in both Epcam[hi] and Epcam^{−} cells, but not in TS cells, whereas TGC (*Prl3d1*) and Sp (*Tpbpa*) markers were absent from both Epcam[hi] and TS cells (Figure 1F). These data suggested that Epcam^{hi} cells are primed for differentiation to labyrinth trophoblasts.

Epcam[hi] Cells Represent Multipotent Labyrinth Trophoblast Progenitors

To define the ability of Epcam^{hi} cells to differentiate into labyrinth trophoblasts, magnetic-activated cell-sorted Epcam^{hi} cells were cultured on OP9 stroma. OP9 cells highly express *Vcam1*, a ligand for integrin α4 (Itga4), which is expressed both in Epcam^{hi} cells (Figure 2A) and on the basal surface of the chorion at the time of chorioallantoic fusion (Stecca et al., 2002). The differentiation potential of Epcam^{hi} cells was compared to that of TS cells, which upregulate markers for the SynT, Sp, and TGC lineages after removal of Fgf4 (Tanaka et al., 1998). After 7 days of culture on OP9, Epcam^{hi} cells maintained the expression of SynT transcription factors *Dlx3* and *Ovol2* and upregulated the mature SynT markers *Mct1* (SynT-I) and *Mct4* (SynT-II; Nagai et al., 2010; Figure 2B) to greater levels than differentiated TS cells, confirming the ability of Epcam^{hi} cells to efficiently generate SynT. Moreover, after 7 days in culture, E-cadherin[+] (Cdh1) cells with multiple nuclei (> 20) were observed (Figure 2C), suggesting that SynT derived from Epcam^{hi} cells can form syncytia in vitro. Costaining with CD9 confirmed that the multinucleated cells were trophoblasts (Figure 2D). Interestingly, expression of sTGC markers *Ctsq* and *Prl3b1* also increased by 7 days of culture, suggesting that Epcam^{hi} cells also differentiate into labyrinth sTGC in vitro (Figure 2B). In contrast, cultured Epcam^{hi} cells evidenced minimal expression of TGC and Sp markers, implying that their differentiation potential is restricted to labyrinth trophoblasts. These data nominated Epcam^{hi} cells as labyrinth trophoblast progenitor cells (LaTP) that can give rise to SynT-I, II, and sTGC.

We next asked if Epcam^{hi} cells are clonally linked to SynT and sTGC in vivo. Tamoxifen-inducible *Rosa26-CreER[T2]* mice were crossed with *Rosa26-Rainbow* reporter strain (Rinkevich et al., 2011), in which all cells express GFP until Cre-mediated recombination induces one of the three other fluorescent proteins (mCherry, mOrange, and mCerulean; Figures 2E and 2F). 4-OH tamoxifen was injected at E9.5 when labyrinth morphogenesis begins, and placentas were analyzed at E12.5 when Epcam^{hi} cells and differentiated SynT and sTGC are present. To facilitate clonal analysis, the dose of 4-OH tamoxifen was titrated to induce rare recombination in trophoblasts. While individual cells marked with mCherry, mOrange, or mCerulean were found in all
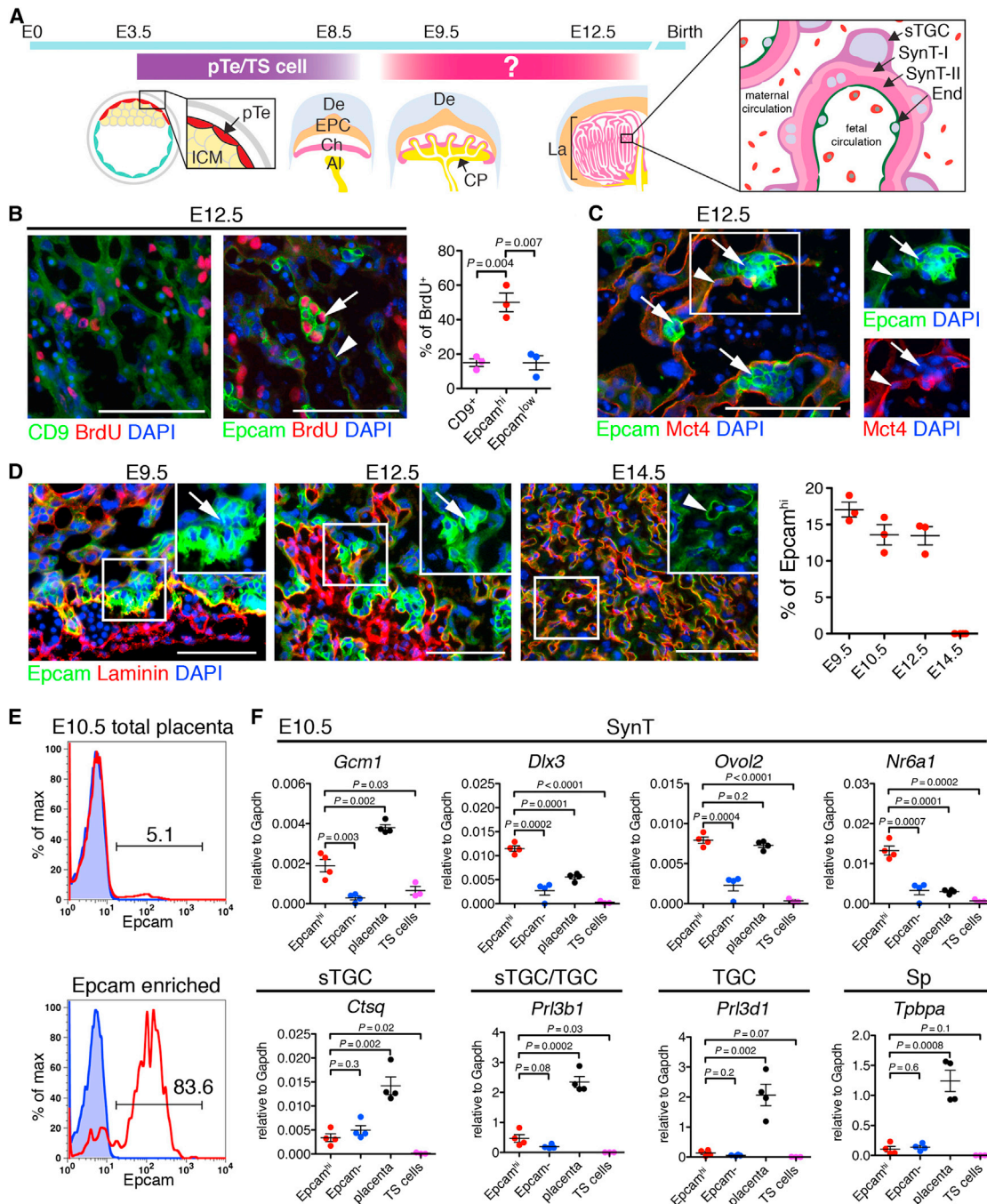
Figure 1. Epcam^hi Cells Are Candidate LaTP Cells

(A) Schematic depicting the development of the mouse placenta. Polar trophectoderm (pTe) develops into ectoplacental cone (EPC) and chorion (Ch). Trophoblast stem (TS) cells can established from trophoectoderm/placenta before E8.5, however, TS cells disappear after chorioallantoic fusion, suggesting that yet unidentified progenitors are responsible for labyrinth development. The labyrinth (La) contains three trophoblast cell types: SynT-I, SynT-II, and sinusoidal trophoblast giant cells (sTGCs). The SynT-II layer is facing fetal endothelium (End), and the sTGC is facing maternal blood. ICM, inner cell mass; De, decidua; Al, allantois; CP, chorionic plate.

(B) Identification of Epcam as a marker for proliferating trophoblasts. Sections from E12.5 placental labyrinth were stained with CD9 or Epcam. DNA synthesis was visualized by BrdU incorporation. Arrow, Epcam^hi cluster. Arrowhead, SynT. Scale bar, 100 μm.

(C) Correlation of SynT-II differentiation marker, Mct4, with low Epcam expression in SynT-II (arrowhead). Arrow, Epcam^hi cluster. Scale bar, 100 μm.

(D) Kinetic analysis of the frequency of Epcam^hi cells in midgestation placentas. Scale bar, 100 μm.

(E) Enrichment of Epcam^hi cells from E10.5 placenta using magnetic bead separation.

(F) Quantitative analysis of the expression of trophoblast subtype-specific genes in Epcam^hi-enriched cells.
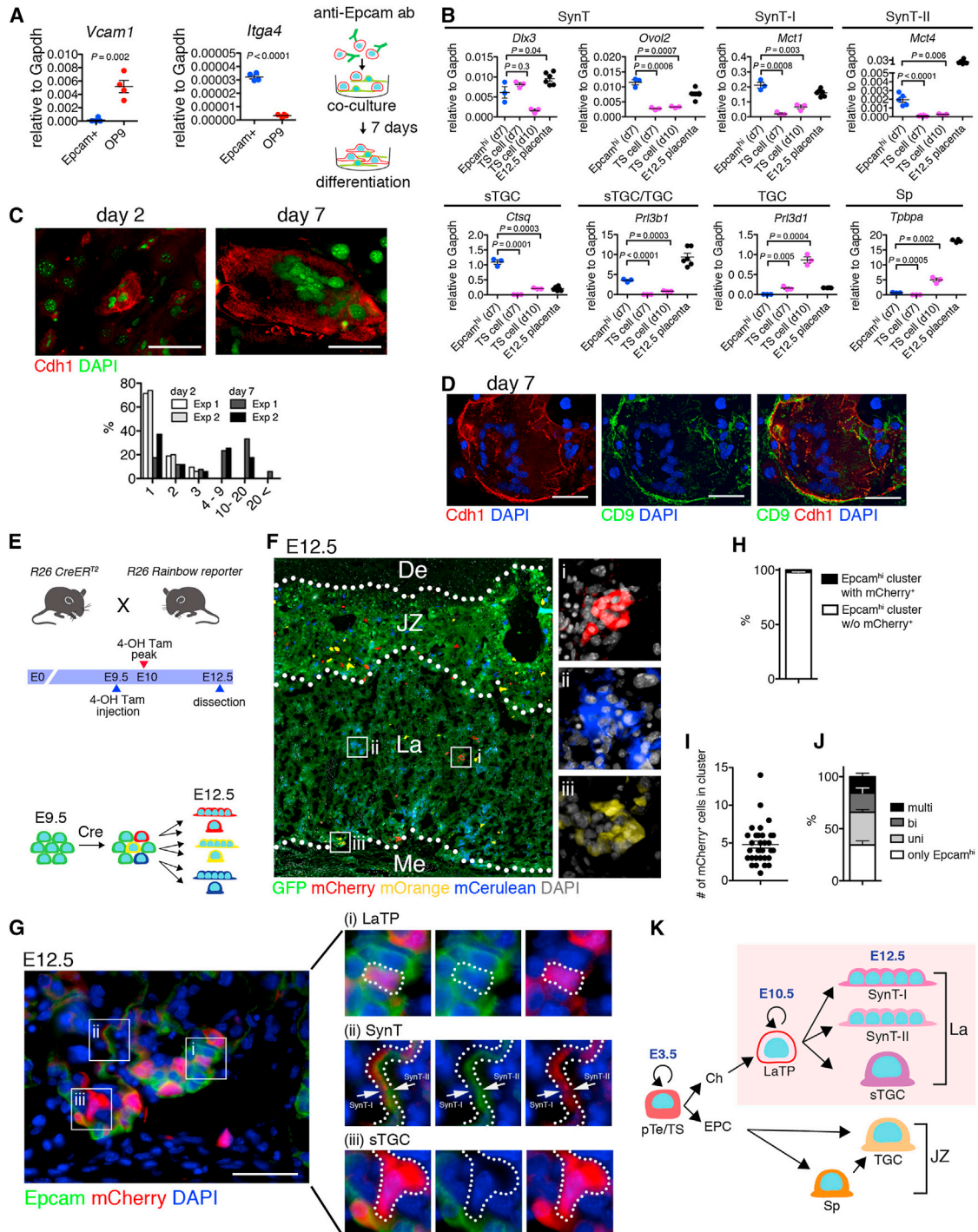
All error bars indicate SEM. See also Figure S1.

Figure 2. Epcam^hi Cells Represent Multipotent LaTPs

(A) Schematic for analysis of the developmental potential of Epcam^hi cells in vitro. Epcam^hi cells from E10.5 placenta were enriched using magnetic beads and cocultured with OP9 for 7 days. qRT-PCR documents the expression of *Itga4* in Epcam^hi cells and *Vcam1* in OP9.

(B) qRT-PCR showing the maintenance of SynT-specific genes and upregulation of markers for differentiated SynT-I and -II and sTGC in Epcam^hi cultures after 7 days.

(C) Documentation of increased frequency of Cdh1^+ SynT with multiple nuclei after 7 days in culture.

(D) Documentation that Cdh1^+ multinucleated cells coexpress trophoblast marker CD9.

(E) Schematic for in vivo clonality analysis. *Rosa26 (R26) Rainbow* reporter mice were mated with *R26 CreER^T2* mice. At E9.5, Cre-mediated gene deletion was induced by injection with 4OH-tamoxifen, and embryos were dissected at E12.5.

(F) Fluorescence image indicating that Cre-mediated gene recombination induces multi-color labeling and establishment of clones of labeled cells in the labyrinth. JZ, junctional zone; La, labyrinth; Me, mesenchyme.

(legend continued on next page)

parts of the fetal placenta, the labyrinth contained several clusters of cells marked with the same color (Figure 2F). To investigate differentiation potential of cells in individual clones, mCherry-labeled clusters were chosen for further analysis (Figure 2G). Of all Epcam^{hi} cell clusters, 2.2% ($\pm$ 0.4) harbored mCherry$^+$ Epcam^{hi} cells (Figure 2H), with each cluster containing on average 4.8 ($\pm$ 2.6) mCherry-labeled trophoblasts (Figure 2I). Quantitative analysis indicated that 15.8% ($\pm$ 4.1) of mCherry-labeled clusters were multipotent and contained labeled clones with Epcam^{hi} LaTP, Epcam$^{low/neg}$ SynT, and Epcam^{neg} sTGC (Figures 2G and 2J). Comparable results of clonal association of Epcam^{hi} LaTP with SynT and sTGC were obtained using *Rosa26-YFP* reporter mice (Figures S2A–S2F). Costaining for Epcam, Cytokeratin, and Mct4 further confirmed labeling of all labyrinth trophoblast subtypes within YFP$^+$-labeled Epcam^{hi} LaTP clusters (Figure S2G). Together, these data suggest that Epcam^{hi} cells are LaTPs that generate all labyrinth trophoblast subtypes in vivo (Figure 2K).

c-Met Signaling Directly Regulates Labyrinth Trophoblast Development

To identify regulators for LaTP, we searched for mouse models with labyrinth defects; the Hgf receptor c-Met was identified as a candidate. We first analyzed the placental defect in *c-Met* KO embryos generated by deleting the conditionally targeted *c-Met* locus (Huh et al., 2004) in the germline (g-KO). Lethality of *c-Met* g-KO embryos occurred by E14.5, as reported for *Hgf* and *c-Met* KO embryos (Bladt et al., 1995; Schmidt et al., 1995; Uehara et al., 1995). No macroscopic defects were observed in placentas or embryos until E12.5, when *c-Met* g-KO placentas and embryos exhibited decreased size and hypocellular fetal liver (FL; Figures S3A–S3D). *c-Met* g-KO placentas had a thinner labyrinth (La) while the JZ composed of Sp and TGC was unaffected (Figure 3A), confirming that placental defects were limited to the labyrinth.

To assess whether loss of Hgf/c-Met signaling in placental trophoblasts alone is sufficient to cause the defects in the placenta and the fetus, we generated trophoblast-specific *c-Met* KO (t-KO) embryos by deleting the *c-Met* gene in trophoblasts using a lentiviral Cre (Figure 3B; Chhabra et al., 2012). *UbiC-Cre-GFP* lentiviral vector was injected under the zona pellucida (ZP) of *c-Met*$^{fl/fl}$ blastocysts, while *c-Met*$^{fl/+}$ blastocysts and untransduced *c-Met*$^{fl/fl}$ blastocysts served as controls. Strikingly, trophoblast-specific *c-Met* deletion mimicked the phenotype of *c-Met* g-KO mutants, resulting in reduced placental labyrinth size and poorly developed branching structure (Figure S3E), IUGR of the embryo (Figures 3C and 3D), and lethality by E14.5 (data not shown). Moreover, loss of *c-Met* in placental trophoblasts alone was sufficient to cause hypocellularity of the FL (Figure S3F). Importantly, transduction of *c-Met*$^{fl/+}$ blastocysts did not show any phenotype in the embryo or the placenta

(data not shown). These findings indicate that trophoblast-specific loss of c-Met causes both labyrinth and FL hypoplasia and IUGR of the embryo.

To examine how c-Met regulates labyrinth development, we conducted Affymetrix microarray analysis on wild-type (WT) and *c-Met* g-KO CD9$^+$ labyrinth trophoblasts. We identified 1,294 genes as downregulated and 1,221 genes as upregulated in *c-Met*-deficient trophoblasts (> 2-fold, p < 0.05; Tables S1 and S2; Figure S3G). The GO category "placenta development" included genes regulating labyrinth development (Figure 3E; Figure S3G). qRT-PCR confirmed reduced expression of SynT genes (*Gcm1, Dlx3, Ovol2, Cebpa,* and *Tead3*; Natale et al., 2006) in *c-Met* g-KO labyrinth trophoblasts (Figure 3F). qRT-PCR of all E12.5 placentas showed that there was no reduction in labyrinth sTGC- (*Ctsq* and *Prl3b1*), TGC- (*Prl3b1, Limk1, Limk2,* and *Hand1*), or Sp-specific genes (*Tpbpa* and *Nodal*; Figure 3G; (Watson and Cross, 2005; Natale et al., 2006). These data further indicated that c-Met signaling specifically regulates labyrinth trophoblast development.

c-Met Sustains Proliferation of LaTP in Midgestation Placenta

The selective suppression of SynT genes and the morphological defects in the placental labyrinth raised the hypothesis that c-Met signaling regulates the emergence, maintenance, and/or differentiation of LaTP. qRT-PCR documented the expression of *c-Met* in both Epcam^{hi} LaTP and CD9^{hi} Epcam$^{low/neg}$ SynT, whereas the mature SynT marker *Mct4* was expressed at a higher level in SynT (Figure 4A). The frequency of Epcam^{hi} cells in *c-Met* g-KO placenta was comparable to that of WT at E9.5, but dramatically decreased from E10.5 onward (Figure 4B). These data suggested that c-Met signaling is not required for specification of LaTP, but rather for their maintenance through midgestation.

The most highly enriched GO categories among genes downregulated in *c-Met*-deficient placentas were related to "cell cycle" (Figures S3G and S4A). qRT-PCR confirmed downregulation of several genes required for cell division, including *Ccna2, Ccne1, Ccne2, Chek1,* and *Cdc45* (Figure 4C). BrdU incorporation assay verified significant reduction in actively proliferating Cytokeratin$^+$ trophoblasts in both *c-Met* g-KO and t-KO placentas at E12.5 (Figure S4B), whereas no difference in DNA fragmentation was observed (Figure S4C), suggesting that defective proliferation rather than apoptosis underlies labyrinth hypoplasia in *c-Met*-deficient placentas. Costaining for phospho-Histone H3 (PH3), a marker of mitosis, and Epcam showed no significant difference in mitotic activity between WT and *c-Met* g-KO Epcam^{hi} LaTP at E9.5, whereas their proliferation was dramatically decreased E10.5 onward (Figure 4D). These data implied that c-Met signaling is required to sustain the proliferation of LaTP in midgestation.

To verify that reduced proliferation of c-Met-deficient LaTP is not caused by indirect effects from other tissues, c-Met signaling

(G) Documentation of multilineage differentiation in a cluster of mCherry-labeled trophoblasts. (i) Epcam^{hi} (LaTP), (ii) SynT (Epcam$^{low/neg}$), and (iii) sTGC (Epcam^{neg} with large nuclei).

(H) Analysis of the frequency of clusters containing mCherry-labeled Epcam^{hi} cells documenting infrequent labeling of clusters with the same fluorescent color.

(I) Average number of mCherry$^+$ cells in a labeled cluster documenting the establishment of multicellular, labeled clones.

(J) Differentiation potential of mCherry-labeled cells documenting the presence of clones with Epcam^{hi} LaTP and all labyrinth trophoblast subtypes.

(K) Schematic representing the hierarchy of trophoblast lineage differentiation. LaTP gives rise to all types of labyrinth trophoblasts, but not Sp or TGC.

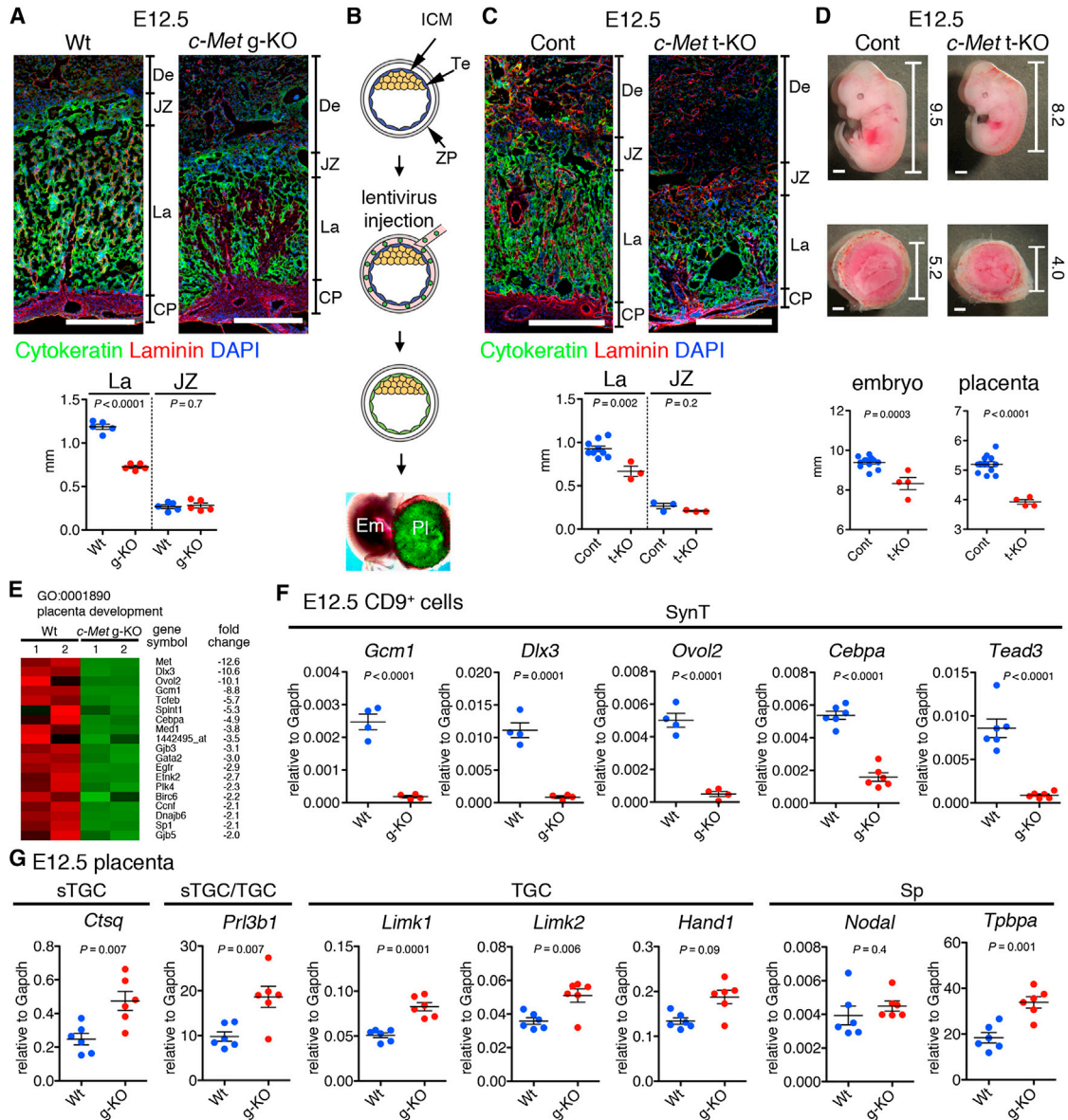All error bars indicate SEM. See also Figure S2.

Figure 3. Loss of c-Met Signaling in Trophoblasts Induces Placental Labyrinth Hypoplasia and IUGR

(A) IF for Cytokeratin (green, trophoblast), Laminin (red, mesenchymal cell), and DAPI (blue, nuclei) on WT and *c-Met* germline KO (g-KO) placenta at E12.5 showing La-specific hypoplasia in *c-Met* g-KO placenta. Scale bar, 500 μm.

(B) Generation of trophoblast-specific *c-Met* KO (t-KO) embryos. Injection of *Cre-GFP* lentivirus under the zona pellucida (ZP) induces Te-specific gene deletion. ICM, inner cell mass; Te, trophectoderm.

(C) Trophoblast-specific *c-Met* gene deletion induces placental labyrinth hypoplasia.

(D) Representative images of *c-Met*fl/fl and *c-Met* trophoblast-specific KO (t-KO) embryos and placentas. Numbers indicate size (in millimeters) of each embryo and placenta. Scale bar, 1 mm.

(E) Heatmap representing differential expression of genes related to placental development (>2.0-fold, p < 0.05) in WT versus *c-Met* g-KO CD9+ trophoblasts.

(F) qRT-PCR for SynT-specific genes on E12.5 WT and *c-Met* g-KO CD9+ trophoblasts. The mean of biological replicates normalized to *Gapdh* is shown.

(G) qRT-PCR for sTGC, TGC, and Sp-specific genes in E12.5 placenta.

All error bars indicate SEM. See also Figure S3 and Tables S1 and S2.

was blocked in LaTP culture using c-Met inhibitor PHA-665752 (Christensen et al., 2003). Inhibition of c-Met signaling impaired the proliferation of Epcam+ cells in culture without increasing apoptosis (Figures 4E and 4F), demonstrating a cell autonomous role for c-Met in sustaining the proliferation of LaTP and/or their progeny.

c-Met Signaling Is Essential for the Establishment of Labyrinth Exchange Interface

Because the expression analysis of *c-Met*-deficient placentas had indicated a dramatic reduction of labyrinth trophoblast-specific transcription factors, we investigated whether c-Met signaling is required for the differentiation of LaTP into SynT
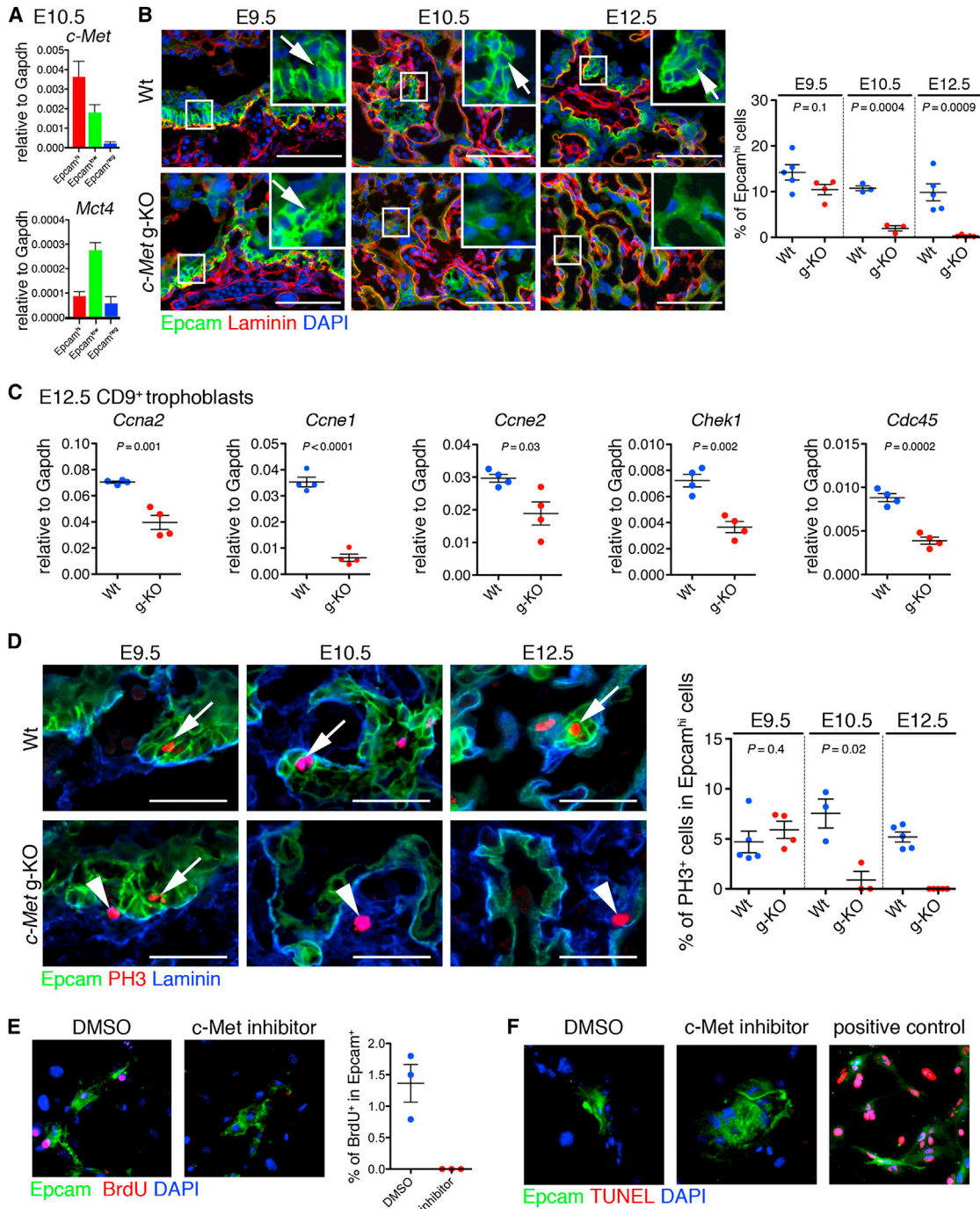
Figure 4. c-Met Signaling Regulates the Maintenance of LaTP

(A) qRT-PCR documenting the expression of *c-Met* in both Epcam[hi] LaTP and Epcam[low] SynT.

(B) IF for Epcam (green) and Laminin (red) on WT and *c-Met* g-KO placenta at E9.5, E10.5, and E12.5 documenting loss of Epcam^{hi} cells in c-Met-deficient placenta after E9.5. Arrows, Epcam^{hi} cells adjacent to laminin^{+} mesenchymal cells. Scale bar, 100 μm.

(C) qRT-PCR analysis of gene expression in CD9^{+} trophoblast from WT and *c-Met* g-KO placentas verifying downregulation of cell cycle regulators.

(D) IF for Epcam (green), phospho-Histone-H3 (PH3, red) and laminin (blue) on WT and *c-Met* g-KO placenta at E9.5, E10.5, and E12.5 documenting premature loss of proliferative LaTP in c-Met-deficient placenta. Arrows, PH3^{+} Epcam^{hi} cells. Arrowheads, PH3^{+} Epcam^{−} cells. Scale bar, 50 μm.

(E) Treatment of cultured LaTP with c-Met inhibitor documents reduced BrdU incorporation in Epcam^{+} cells. Epcam (green), BrdU (red), DAPI (blue).

(F) Treatment of cultured LaTP with c-Met inhibitor documenting no difference in cell death of Epcam^{+} cells. Epcam (green), TUNEL (red), DAPI (blue). Positive control, cells treated with DNase I.

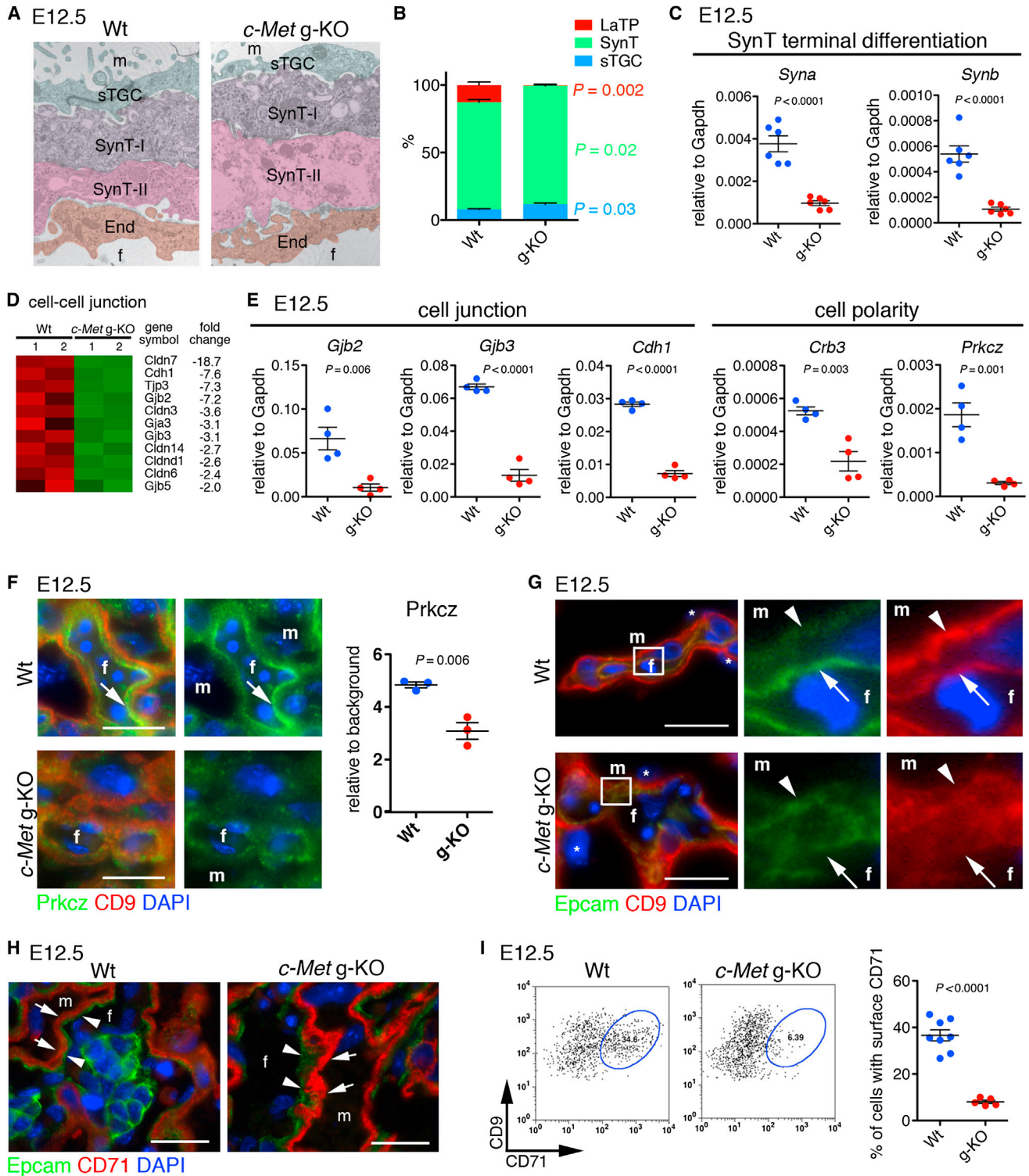All error bars indicate SEM. See also Figure S4.

Figure 5. c-Met Signaling Is Dispensable for SynT and sTGC Specification but Essential for SynT Terminal Differentiation and Cell Polarity

(A) Electron microscopy showing trilaminar structure of labyrinth trophoblasts (SynT-I, SynT-II, and sTGC) in WT and *c-Met* g-KO placentas.

(B) Quantitative analysis for trophoblast subtypes.

(C) qRT-PCR showing decreased expression of *Syna* and *Synb* in E12.5 *c-Met* KO CD9^{+} trophoblasts.

(D) Heatmap of cell-cell junction genes differentially expressed between WT and *c-Met* g-KO CD9^{+} trophoblasts.

(E) qRT-PCR showing reduced expression of cell-cell junction and cell polarity genes in *c-Met* g-KO trophoblasts.

(legend continued on next page)

and/or sTGC. Electron microscopy indicated that the trilaminar trophoblast structure consisting of SynT-II, SynT-I, and sTGC was established in *c-Met* g-KO placenta (Figure 5A). Costaining for Mct4 (SynT-II) and CD9 (both SynT subtypes) confirmed the presence of both SynT-I and -II in *c-Met* g-KO placentas (Figure S5A). Quantification of the relative frequencies of labyrinth trophoblasts in *c-Met* g-KO placentas at E12.5 revealed a slight decrease of SynT and increase of sTGC, while Epcam^{hi} cells were nearly undetectable (Figure 5B). Nevertheless, despite the presence of both SynT-I and SynT-II in *c-Met* g-KO placentas, the expression of *Syncytin-a* (*Syna*) and *-b* (*Synb*) that mark terminally differentiated SynT-I and SynT-II, respectively, was dramatically reduced, suggesting a defect in terminal differentiation (Figure 5C). Microarray analysis and qRT-PCR revealed reduced expression of genes encoding tight junction proteins *Cldn3*, *6*, *7*, and *14*, and *Tjp3*, adherence junction proteins (*Cdh1* [*E-cadherin*]), and gap junction proteins *Gjb2* (*Cx26*) and *Gjb3* (*Cx31*), which are highly expressed in differentiated SynT and critical for labyrinth development (Gabriel et al., 1998; Plum et al., 2001; Figures 5D and 5E).

Epithelial cells exhibit apical-basolateral polarity that is essential for organ development and function (Martin-Belmonte and Perez-Moreno, 2012). Closer examination of the CD9 staining pattern in c-Met-deficient trophoblasts revealed that although CD9 was localized on both the fetal side of SynT-II and maternal (apical) side of SynT-I in WT placentas (Figure S5A), it was diffusely localized in *c-Met* g-KO SynT, suggesting that c-Met signaling regulates SynT cell polarity. Microarray analysis and qRT-PCR revealed downregulation of polarity genes *Crb3* and *aPKCζ* (*Prkcz*) in *c-Met* g-KO trophoblasts (Figure 5E). No statistically significant reduction was observed by qRT-PCR for *Pard3* and *Pard6b* (data not shown), which form a complex with Prkcz to establish cell polarity in many cell types (Martin-Belmonte and Perez-Moreno, 2012). Quantitative IF analysis documented reduction of Prkcz protein in *c-Met* KO placenta (Figure 5F). Moreover, while Prkcz was expressed at the fetal side of SynT-II in WT placenta (Figure 5F), a more diffuse expression of the residual Prkcz protein was observed in *c-Met* g-KO SynT-II. Likewise, although Epcam expression in SynT in WT placenta was confined to the membrane of the fetal (basal) side of SynT-II (Figure 5G), in *c-Met* g-KO placenta, Epcam was diffusely expressed. In the yolk sac, Epcam was distributed on the basolateral membrane and CD9 was abundantly expressed at the apical surface in both WT and *c-Met* g-KO (Figure S5B), indicating that cell polarity was disrupted only in the placenta. These data demonstrated a pivotal role for c-Met signaling in the establishment of apical-basolateral cell polarity during SynT differentiation.

Transplacental iron transport from the mother is critical for normal fetal development. Serum iron is bound to transferrin (Trf), and is taken up by transferrin receptor (CD71) via endocytosis. After iron dissociation, Trf-CD71 complex is recycled to the cell surface (Grant and Donaldson, 2009). CD71 is necessary for fetal development (Levy et al., 1999), and the endocytic recycling of CD71 is tightly regulated by cell polarity machinery (Golachowska et al., 2010). IF and FACS analysis showed that in WT placenta, CD71 is expressed in both the cytoplasm and cell surface of SynT-I (Figures 5H and 5I). However, although IF demonstrated abundant cytoplasmic expression of CD71 in *c-Met*-deficient SynT-I (Figure 5H), FACS analysis revealed drastic reduction of surface CD71 (Figure 5I). These data suggested that impaired cell polarity in the *c-Met* KO placenta causes abnormal subcellular distribution of CD71 and other proteins required for fetal-maternal transport.

c-Met Signaling Is Required for the Maintenance of *Gcm1* Expression in Midgestation Placenta

Expression analysis of c-Met-deficient trophoblasts had indicated a dramatic reduction of transcription factors regulating SynT development; the analysis of trophoblast subtypes in the labyrinth indicated that both SynT-I and SynT-II were specified in the absence of c-Met, but their terminal differentiation was compromised. To investigate whether c-Met signaling in trophoblasts is directly required for the expression of transcription factors regulating labyrinth morphogenesis, cultured Epcam^{hi} cells were treated with c-Met inhibitor. qRT-PCR revealed that blocking c-Met signaling in vitro in LaTP and their progeny resulted in a drastically reduced expression of *Gcm1*, but not *Ovol2*, *Dlx3*, or *Tead3* (Figure 6A). IF verified the reduction of Gcm1 LaTP cultures treated with the c-Met inhibitor (Figure 6B).

Gcm1 is a transcription factor essential for labyrinth morphogenesis and SynT differentiation (Anson-Cartwright et al., 2000; Simmons et al., 2008). While *Gcm1* is highly expressed in differentiated, postmitotic SynT-II, *Gcm1* expression has also been reported in the chorion at E8.5 and in putative precursors of the labyrinth trophoblasts at E9.5 (Basyuk et al., 1999; Hunter et al., 1999; Stecca et al., 2002). qRT-PCR analysis of FACS-sorted Epcam^{hi} LaTP and Epcam^{low} CD9^{hi} SynT cells from E10.5 placenta documented *Gcm1* expression in both fractions (Figure S6A). In situ hybridization evidenced the expression of *Gcm1* also in Epcam[hi] LaTP at E10.5 (Figure S6B), whereas by E14.5, *Gcm1* expression was largely confined to SynT-II (Figure S6C). IF suggested that Gcm1 is expressed in some Epcam[hi] LaTP that are undergoing mitosis (Figure S6D). These data imply that *Gcm1* expression is not restricted to differentiated, postmitotic SynT but begins already at the level of LaTP.

To investigate whether Gcm1 expression is required for the emergence and/or differentiation of LaTP, the expression of

(F) IF for Prkcz (green) and CD9 (red) showing polarized localization of Prkcz protein in fetal side of SynT-II in WT placenta (arrow), and diffuse and decreased expression of Prkcz in *c-Met* g-KO placenta. DAPI (blue, nuclei).

(G) IF for Epcam (green), CD9 (red), and DAPI (blue) on WT and *c-Met* g-KO placenta at E12.5. Arrows indicate fetal side of SynT-II and arrowheads indicate apical membrane of SynT-I. m, maternal blood space; f, fetal vascular lumen.

(H) IF for Epcam (green), CD71 (red), and DAPI (blue) on placental section at E12.5. Expression of cytoplasmic CD71 in SynT-I (arrowheads) is observed in both WT and *c-Met* g-KO placenta.

(I) FACS analysis indicating reduced surface expression of CD71 on SynT in *c-Met* g-KO placentas.

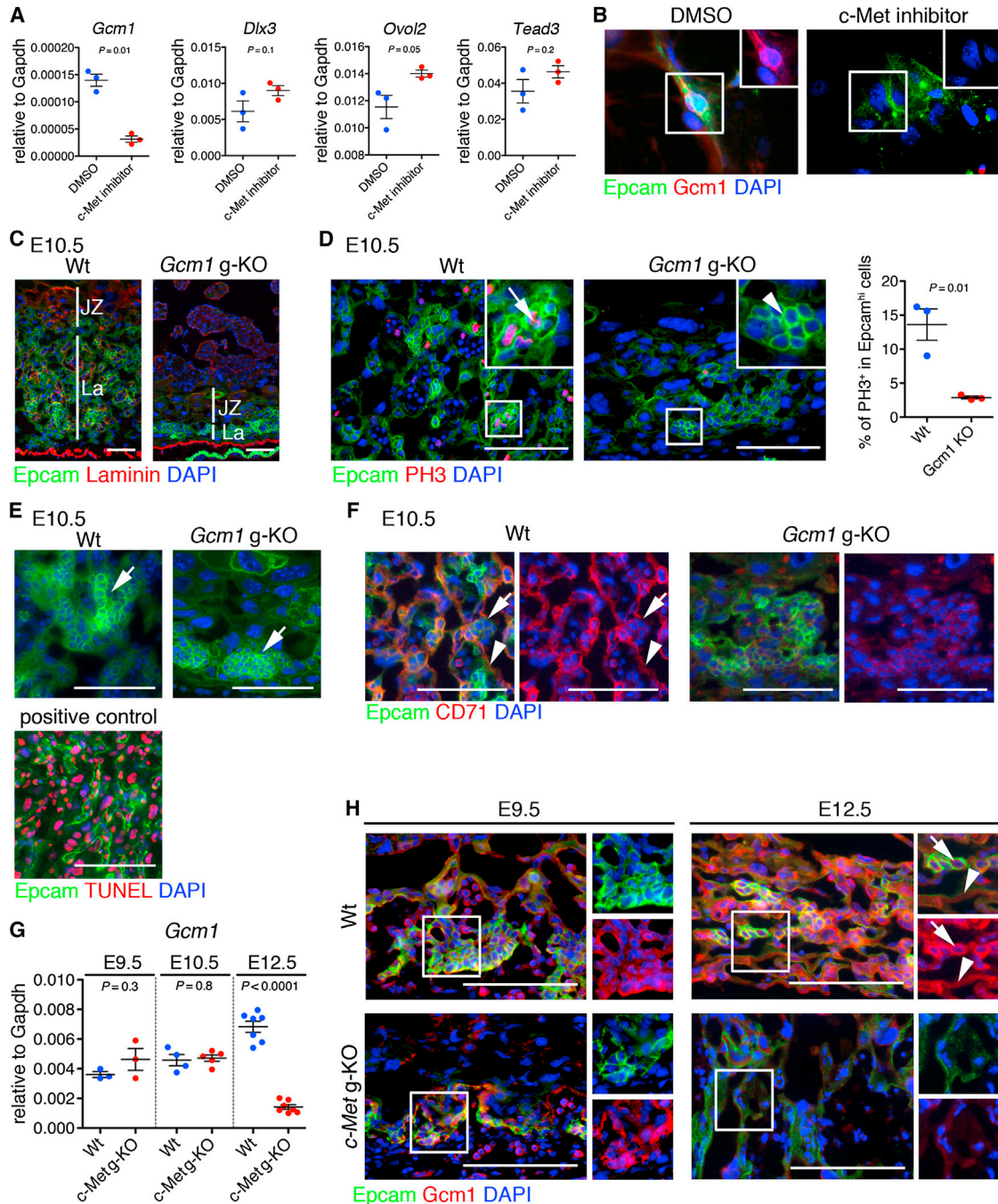All error bars indicate SEM. See also Figure S5.

Figure 6. c-Met Signaling Is Required to Maintain Gcm1 Expression in Midgestation Placenta

(A) qRT-PCR demonstrating loss of *Gcm1* expression upon treatment of cultured LaTP with c-Met inhibitor.

(B) IF documenting loss of Gcm1 in Epcam$^+$ cells upon treatment with c-Met inhibitor. Epcam (green), Gcm1 (red), DAPI (blue).

(C) IF documenting reduced labyrinth size in *Gcm1* g-KO placenta. Scale bar, 100 μm. Epcam (green), laminin (red), DAPI (blue).

(D) Phospho-Histone H3 staining documenting reduction of mitotic Epcam^{hi} cells (arrow) in *Gcm1* KO placentas. Arrowheads, PH3 negative Epcam^{hi} cluster. Epcam (green), PH3 (red), DAPI (blue). Scale bar, 100 μm.

(E) TUNEL staining indicating apoptosis is not induced in *Gcm1* g-KO placenta at E10.5. Positive control for Tunel staining is shown below. Epcam (green), TUNEL (red), DAPI (blue). Scale bar, 100 μm.

(F) IF showing absence of CD71$^+$ SynT in *Gcm1* g-KO placenta. Epcam (green), CD71 (red), DAPI (blue). Scale bar, 100 μm.

(G) qRT-PCR and (H) IF documenting loss of Gcm1 expression by E12.5 in *c-Met* g-KO placentas. Epcam (green), Gcm1 (red) DAPI (blue). Scale bar 100 μm. All error bars indicate SEM. See also Figure S6.
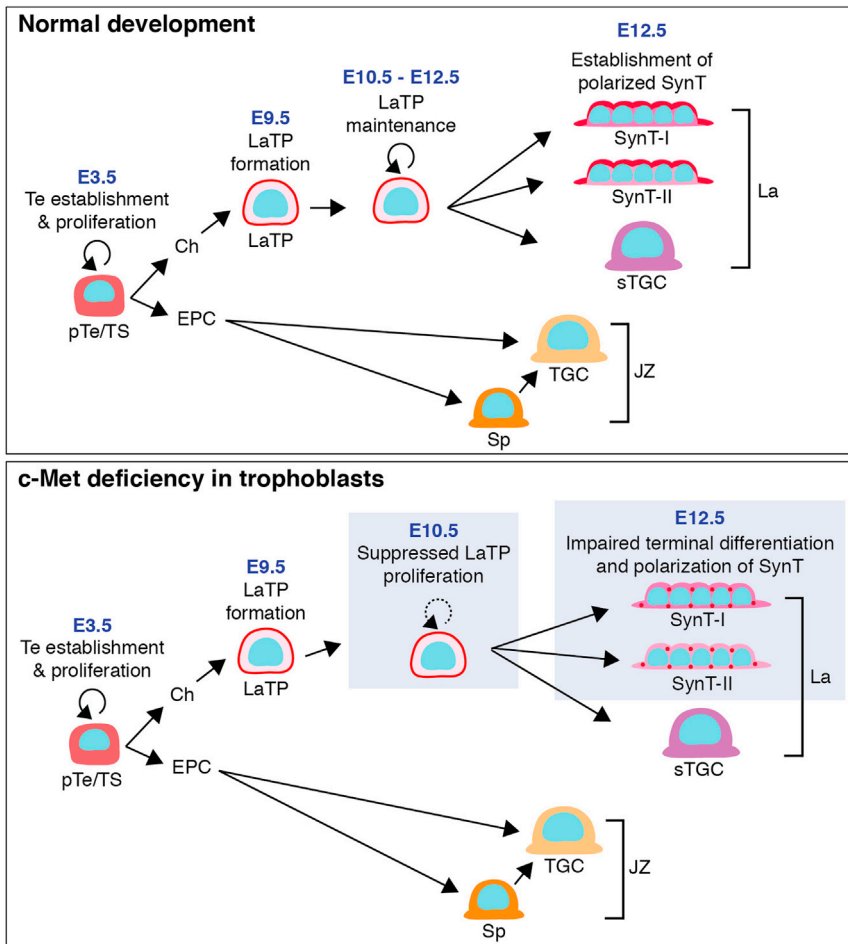
Figure 7. Model for Function of Hgf/c-Met Signaling in the Development of Placental Exchange Interface

LaTPs are responsible for the generation of SynT I and II and sTGC that compose the placental exchange interface. While LaTP can be specified independently of c-Met signaling, c-Met is essential for sustained proliferation of LaTP. c-Met signaling is also required for the establishment of SynT cell polarity. Loss of c-Met signaling results in placental hypoplasia, a compromised exchange interface, and defective fetal development.

DISCUSSION

The stem/progenitor cell hierarchy of the trophoblasts responsible for placental labyrinth morphogenesis and exchange function has been unknown. We discovered that the midgestation mouse placenta harbors Epcam[hi] multipotent labyrinth trophoblast progenitors (LaTP) that differentiate into all labyrinth trophoblast subtypes, SynT-I, SynT-II, and sTGC, in vitro and in vivo. We discovered that c-Met signaling is required for sustained proliferation of LaTP during midgestation and for terminal differentiation and polarization of SynT, which is a prerequisite for a functional placental exchange interface and healthy fetal development (Figure 7).

Clonal analysis using multicolor Rainbow reporter mouse (Rinkevich et al., 2011) revealed that marking individual cells in the placenta results in the generation of multicellular clusters that contain Epcam[hi] LaTP, SynT-I, SynT-II, and sTGC. Although 15.8% of the labeled trophoblast clusters identified at E12.5 (labeled at around E9.5) were multipotent, 34.5% of all labeled the clusters contained only undifferentiated Epcam[hi] LaTP, indicating that they had not started to differentiate at this stage, while the remaining labeled clones were composed of Epcam[hi] LaTP and SynT or sTGC only. Future studies using marking at different time points will reveal whether the differentiation potential of LaTP changes during development. Thus, studies should focus on creating a Cre line that confers LaTP-specific labeling to lineage trace the progeny of LaTP throughout development.

Our data show that both LaTP and SynT express c-Met, while mesenchymal cells derived from the allantois secrete Hgf (Uehara et al., 1995), suggesting paracrine signaling. Abrogation of c-Met signaling disrupted the proliferation of Epcam^{hi} cells both in vivo and in vitro. Nevertheless, our data suggest that Hgf/c-Met signaling is necessary, but not sufficient to support LaTP proliferation and/or SynT differentiation without other niche factors; culture of Epcam^{hi} cells in TS cell conditions or on Matrigel with Hgf failed to support SynT differentiation and maintain Gcm1 expression. However, culture of Epcam^{hi} cells on OP9 mesenchymal stroma, which secretes Hgf and expresses Vcam1 (Malhotra and Kincade, 2009) that is essential

Epcam was assessed in *Gcm1* KO placentas at E10.5, before embryonic death. As reported previously (Anson-Cartwright et al., 2000), the labyrinth layer was much thinner, and no branching morphogenesis was observed (Figure 6C). Notably, *Gcm1* KO placentas harbored Epcam^{hi} cells; however, the frequency of PH3^{+} mitotic Epcam^{hi} cells was drastically reduced (Figure 6D), while no increase in apoptosis was revealed by TUNEL assay (Figure 6E). Moreover, no CD71^{+} differentiating SynT were found in *Gcm1* KO placentas (Figure 6F). These data suggested that complete lack of Gcm1 expression compromises both the proliferation and differentiation of Epcam[hi] LaTP in vivo.

Because the placental phenotype in *Gcm1* KO embryos was much more severe than that in *c-Met* KO embryos, we investigated the kinetics of *Gcm1* expression in c-Met-deficient placentas. At E9.5, there was no difference in the expression of *Gcm1* between *c-Met* deficient and WT placentas, whereas by E12.5, *Gcm1* expression in the mutant trophoblasts was nearly undetectable with IF and qRT-PCR (Figures 6G and 6H). These data suggested that c-Met is not essential for inducing *Gcm1* expression, but rather for maintaining its expression in LaTP and SynT through midgestation. Altogether, these findings identify Gcm1 as a key downstream effector of c-Met signaling, and suggest that its continued expression in LaTP and/or SynT in the midgestation placenta is required for the establishment of a functional placental exchange interface.

for maintaining *Gcm1* expression in placental explant cultures (Stecca et al., 2002), facilitated the maintenance/induction of SynT genes and formation of multinucleated syncytia. Cultured Epcam^hi LaTP also induced genes specific for labyrinth sTGC, which have been implicated as key hematopoietic niche cells (Chhabra et al., 2012). These data imply that the Epcam^hi cell culture may be used to study the trophoblast subtypes that establish the exchange interface and the hematopoietic niche in the placental labyrinth. Future work will be needed to define distinct niche components to direct the differentiation of LaTP to specific labyrinth trophoblast subtypes and to investigate whether LaTP can be sustained in an undifferentiated state in culture.

Although previous studies had associated defective c-Met signaling with disrupted labyrinth development, the underlying mechanisms were unknown. Our data revealed a critical role for c-Met in the maintenance of *Gcm1* expression in midgestation placenta whereas the initial induction of *Gcm1* occurs independently of c-Met. This finding helps explain the less drastic placental defect in *c-Met* KO embryos than in *Gcm1* KO embryos, because a complete lack of *Gcm1* disrupted labyrinth morphogenesis and SynT differentiation entirely, causing embryonic death by E10.5 (Anson-Cartwright et al., 2000). Analysis of *Gcm1* KO placentas suggested that Epcam^hi LaTP can be specified in the absence of *Gcm1,* but their proliferation and differentiation is disturbed. In contrast, loss of *c-Met* did not abolish the expression of *Gcm1* or cause macroscopic defects in *c-Met* KO labyrinth until E12.5, when LaTP were extinguished and *Gcm1* expression dropped to undetectable levels. Altogether, these data suggest that the specification of LaTP is induced by a c-Met- and Gcm1-independent mechanism; however, c-Met is required for SynT terminal differentiation and establishment of the placental exchange interface, which may at least in part be linked to the requirement of c-Met signaling to maintain Gcm1 expression.

Previous studies have shown that Gcm1 is highly expressed in postmitotic cells in the labyrinth and that overexpression of Gcm1 induces cell cycle arrest (Hughes et al., 2004). Our data also confirmed high expression of Gcm1 in differentiated SynT-II. In addition, the ability to distinguish undifferentiated LaTP in the labyrinth by Epcam^hi staining identified a small population of proliferative LaTP that also express Gcm1. Because TS cells do not express Gcm1, it is plausible that expression of Gcm1 is important for LaTP commitment to the SynT lineage. To verify if Gcm1 governs the differentiation of LaTP to SynT, and/or is directly involved in maintaining LaTP proliferation, further studies deleting Gcm1 in a cell-type-specific and temporal manner will be required.

As with mouse placenta, little is known about the stem/progenitor cell hierarchy in the human placenta. Despite similarities in molecular regulation, the mouse and human placentas are macroscopically distinct (Georgiades et al., 2002). Thus, the direct relevance of the findings of mouse LaTP to human placental progenitor biology needs to be explored separately. Recent studies documented that the chorionic membrane of the first trimester human placenta can serve as a source of trophoblast progenitor cell lines that highly express *GCM1* and upregulate *SYNCYTIN* after differentiation in vitro (Genbacev et al., 2011), raising the hypothesis that they originate from a precursor that has a parallel function in establishing the placental exchange interface as the mouse LaTP.

Differentiated SynT form a "placental barrier" that tightly regulates the passage of substances between the maternal and fetal circulations (Kokkinos et al., 2010). We showed that while c-Met-deficient LaTP can form all labyrinth trophoblast subtypes, c-Met is necessary for terminal differentiation into polarized SynT. Trophoblast cell lines have provided a useful tool to study cell polarity in vitro (Sivasubramaniyam et al., 2013); however, little is known about the direct functional consequences of disrupted SynT cell polarity in vivo. In addition to the low expression of key cell polarity molecules and the inability to achieve polarized localization of SynT surface proteins in *c-Met* KO placentas, the surface localization of transferrin receptor (CD71), required for transplacental iron transfer, on SynT-I was impaired. Future studies are needed to define the mechanisms as to how the disturbed placental exchange *c-Met*-deficient embryos causes fetal liver hypocellularity, IUGR, and death of the fetus. Thus, c-Met-deficient placentas not only offer a unique in vivo model to investigate how the apical-basolateral polarity and bidirectional transport in SynT is established, but may also help uncover the etiology of pregnancy complications related to placental transport function.

Reduced expression of Hgf has been observed in human placentas from preeclampsia and IUGR pregnancies (Furugori et al., 1997; Somerset et al., 1998), and in vitro studies demonstrated that Hgf activates invasion of human trophoblasts (Kauma et al., 1999; Nasu et al., 2000), providing evidence for MET signaling in placental development and disease in human. Moreover, similar to many human placenta-related disorders such as spontaneous abortion, premature delivery, IUGR, and preeclampsia that are accompanied by placental inflammation (Young et al., 2010), *c-Met* deficiency in trophoblasts induced inflammation and macrophage infiltration in the placenta (unpublished data). Although the mechanisms that trigger inflammation in c-Met-deficient trophoblasts are still unknown, this may be related to downregulation of cell-cell junction molecules and/or defective cell polarity in SynT that compromise fetal-maternal barrier function. Moreover, c-Met is constitutively activated in human choriocarcinoma, and Hgf stimulates the proliferation of choriocarcinoma cells (Saito et al., 1995; Takayanagi et al., 2000). *c-Met* also regulates the proliferation and migration of various other cancer cells and stem cells (Boccaccio and Comoglio, 2006). Thus, defining how Hgf/c-Met signaling governs the proliferation of stem/progenitor cells such as LaTP and the establishment of cell polarity in their differentiated progeny may have implications to understanding the pathophysiology of other common diseases.

EXPERIMENTAL PROCEDURES

Animals

All procedures with animals were conducted according to the guidelines of the UCLA Animal Research Committee. For LaTP culture, E10.5 pregnant mice (ICR, Taconic) were used. For the in vivo clonality experiments, *Rosa26-Rainbow* reporter or *Rosa26-YFP* reporter mice were mated with *Rosa26-Cre-ER^{T2}* mice. Pregnant females were injected with 0.5 mg 4-OH tamoxifen at E9.5, and tissues were collected at E12.5. *c-Met^{fl/fl}* mice were provided by Dr. Snorri S. Thorgeirsson (NIH, Bethesda, MD, USA; Huh et al., 2004). To generate trophoblast-specific *c-Met* KO embryos, lentiviral

vector-expressing *Cre-Gfp* was microinjected under the ZP of the blastocyst and embryos were transplanted into pseudopregnant females, as shown earlier (Chhabra et al., 2012). For details, see the Supplemental Experimental Procedures. Sections of *Gcm1* KO placentas were provided by Dr. James C. Cross (University of Calgary, Calgary, Canada).

LaTP and TS Cell Culture
E10.5 placenta was digested with 1 mg/ml collagenase and 1 mg/ml dispase. Epcam^{hi} cells were enriched using anti-Epcam antibody and anti-rat IgG magnetic beads. Epcam^{hi} cells were cocultured with mitomycin C-treated OP9 stroma cell with TS medium (RPMI 1640; Invitrogen) containing 20% fetal calf serum (HyClone), 2 mM L-glutamine, 100 U/ml penicillin, 100 μg/ml streptomycin, 1 mM sodium pyruvate, and 100 μM β-mercaptoethanol) with or without c-Met inhibitor, PHA665752 (4 μM, Sigma-Aldrich) for 7 days. TS cells were maintained as described (Tanaka et al., 1998). TS cell differentiation was induced by removing mouse embryonic fibroblast-conditioned medium, Fgf4, and heparin for 7 and 10 days.

Immunofluorescence and In Situ Hybridization
Histology, BrdU incorporation assay, electron microscopy, qRT-PCR, and immunofluorescence were performed as described (Chhabra et al., 2012). For details of the antibodies, see the Supplemental Experimental Procedures. For demonstration of vascular branching, thick placental sections (3 mm) were prepared by vibratome and three-dimensional images were constructed using confocal microscopy. In situ hybridization was performed using digoxigenin (DIG)-labeled RNA antisense or sense probes for *Gcm1* and the alkaline phosphatase reaction (Simmons et al., 2008).

Gene Expression Analysis
For microarray analysis of *c-Met*-deficient trophoblasts, a single cell suspension of E12.5 placentas was stained with PE-conjugated anti-CD9 antibody and CD9⁺ trophoblasts were enriched using anti-PE antibody-magnetic microbeads. Affymetrix MOE430_2.0 microarrays were performed on two independent WT and two *c-Met* g-KO CD9⁺ trophoblasts. Details about microarray analysis and primer sequences (Table S3) are available in the Supplemental Experimental Procedures.

Statistical Analysis
For statistical analysis, Student's unpaired two-tailed t test was used for all comparisons.

ACCESSION NUMBERS
The Gene Expression Omnibus accession number for the microarray data reported in the paper is GSE38342.

SUPPLEMENTAL INFORMATION
Supplemental Information includes Supplemental Experimental Procedures, six figures, and three tables can be found with this article online at http://dx.doi.org/10.1016/j.devcel.2013.10.019.

AUTHOR CONTRIBUTIONS
M.U. conceived the hypothesis, designed and performed the experiments, and analyzed the data. L.K.L., A.C., Y.J.K., Y.W., B.V.H., M.K., P.K., K-I.S., R.A., and M.J. carried out experiments, and R.S. carried out bioinformatics analyses. H.K.A.M. conceived the hypothesis and directed the project. M.U. and H.K.A.M. prepared the manuscript, which all authors edited and approved.

REFERENCES

Anson-Cartwright, L., Dawson, K., Holmyard, D., Fisher, S.J., Lazzarini, R.A., and Cross, J.C. (2000). The glial cells missing-1 protein is essential for branching morphogenesis in the chorioallantoic placenta. Nat. Genet. *25*, 311–314.

Basyuk, E., Cross, J.C., Corbin, J., Nakayama, H., Hunter, P., Nait-Oumesmar, B., and Lazzarini, R.A. (1999). Murine Gcm1 gene is expressed in a subset of placental trophoblastic cells. Dev. Dyn. *214*, 303–311.

Bladt, F., Riethmacher, D., Isenmann, S., Aguzzi, A., and Birchmeier, C. (1995). Essential role for the c-met receptor in the migration of myogenic precursor cells into the limb bud. Nature *376*, 768–771.

Boccaccio, C., and Comoglio, P.M. (2006). Invasive growth: a MET-driven genetic programme for cancer and stem cells. Nat. Rev. Cancer *6*, 637–645.

Chhabra, A., Lechner, A.J., Ueno, M., Acharya, A., Van Handel, B., Wang, Y., Iruela-Arispe, M.L., Tallquist, M.D., and Mikkola, H.K.A. (2012). Trophoblasts regulate the placental hematopoietic niche through PDGF-B signaling. Dev. Cell *22*, 651–659.

Christensen, J.G., Schreck, R., Burrows, J., Kuruganti, P., Chan, E., Le, P., Chen, J., Wang, X., Ruslim, L., Blake, R., et al. (2003). A selective small molecule inhibitor of c-Met kinase inhibits c-Met-dependent phenotypes in vitro and exhibits cytoreductive antitumor activity in vivo. Cancer Res. *63*, 7345–7355.

Furugori, K., Kurauchi, O., Itakura, A., Kanou, Y., Murata, Y., Mizutani, S., Seo, H., Tomoda, Y., and Nakamura, T. (1997). Levels of hepatocyte growth factor and its messenger ribonucleic acid in uncomplicated pregnancies and those complicated by preeclampsia. J. Clin. Endocrinol. Metab. *82*, 2726–2730.

Gabriel, H.D., Jung, D., Bützler, C., Temme, A., Traub, O., Winterhager, E., and Willecke, K. (1998). Transplacental uptake of glucose is decreased in embryonic lethal connexin26-deficient mice. J. Cell Biol. *140*, 1453–1461.

Gekas, C., Dieterlen-Lièvre, F., Orkin, S.H., and Mikkola, H.K.A. (2005). The placenta is a niche for hematopoietic stem cells. Dev. Cell *8*, 365–375.

Genbacev, O., Donne, M., Kapidzic, M., Gormley, M., Lamb, J., Gilmore, J., Larocque, N., Goldfien, G., Zdravkovic, T., McMaster, M.T., and Fisher, S.J. (2011). Establishment of human trophoblast progenitor cell lines from the chorion. Stem Cells *29*, 1427–1436.

Georgiades, P., Ferguson-Smith, A.C., and Burton, G.J. (2002). Comparative developmental anatomy of the murine and human definitive placentae. Placenta *23*, 3–19.

Golachowska, M.R., Hoekstra, D., and van IJzendoorn, S.C. (2010). Recycling endosomes in apical plasma membrane domain formation and epithelial cell polarity. Trends Cell Biol. *20*, 618–626.

Grant, B.D., and Donaldson, J.G. (2009). Pathways and mechanisms of endocytic recycling. Nat. Rev. Mol. Cell Biol. *10*, 597–608.

Hughes, M., Dobric, N., Scott, I.C., Su, L., Starovic, M., St-Pierre, B., Egan, S.E., Kingdom, J.C., and Cross, J.C. (2004). The Hand1, Stra13 and Gcm1 transcription factors override FGF signaling to promote terminal differentiation of trophoblast stem cells. Dev. Biol. *271*, 26–37.

Hunter, P.J., Swanson, B.J., Haendel, M.A., Lyons, G.E., and Cross, J.C. (1999). Mrj encodes a DnaJ-related co-chaperone that is essential for murine placental development. Development *126*, 1247–1258.

Huh, C.G., Factor, V.M., Sánchez, A., Uchida, K., Conner, E.A., and Thorgeirsson, S.S. (2004). Hepatocyte growth factor/c-met signaling pathway

is required for efficient liver regeneration and repair. Proc. Natl. Acad. Sci. USA 101, 4477–4482.

Kauma, S.W., Bae-Jump, V., and Walsh, S.W. (1999). Hepatocyte growth factor stimulates trophoblast invasion: a potential mechanism for abnormal placentation in preeclampsia. J. Clin. Endocrinol. Metab. 84, 4092–4096.

Kokkinos, M.I., Murthi, P., Wafai, R., Thompson, E.W., and Newgreen, D.F. (2010). Cadherins in the human placenta—epithelial-mesenchymal transition (EMT) and placental development. Placenta 31, 747–755.

Levy, J.E., Jin, O., Fujiwara, Y., Kuo, F., and Andrews, N.C. (1999). Transferrin receptor is necessary for development of erythrocytes and the nervous system. Nat. Genet. 21, 396–399.

Malhotra, S., and Kincade, P.W. (2009). Canonical Wnt pathway signaling suppresses VCAM-1 expression by marrow stromal and hematopoietic cells. Exp. Hematol. 37, 19–30.

Maltepe, E., Bakardjiev, A.I., and Fisher, S.J. (2010). The placenta: transcriptional, epigenetic, and physiological integration during development. J. Clin. Invest. 120, 1016–1025.

Martin-Belmonte, F., and Perez-Moreno, M. (2012). Epithelial cell polarity, stem cells and cancer. Nat. Rev. Cancer 12, 23–38.

McQualter, J.L., Yuen, K., Williams, B., and Bertoncello, I. (2010). Evidence of an epithelial stem/progenitor cell hierarchy in the adult mouse lung. Proc. Natl. Acad. Sci. USA 107, 1414–1419.

Morasso, M.I., Grinberg, A., Robinson, G., Sargent, T.D., and Mahon, K.A. (1999). Placental failure in mice lacking the homeobox gene Dlx3. Proc. Natl. Acad. Sci. USA 96, 162–167.

Mould, A., Morgan, M.A., Li, L., Bikoff, E.K., and Robertson, E.J. (2012). Blimp1/Prdm1 governs terminal differentiation of endovascular trophoblast giant cells and defines multipotent progenitors in the developing placenta. Genes Dev. 26, 2063–2074.

Nagai, A., Takebe, K., Nio-Kobayashi, J., Takahashi-Iwanaga, H., and Iwanaga, T. (2010). Cellular expression of the monocarboxylate transporter (MCT) family in the placenta of mice. Placenta 31, 126–133.

Nasu, K., Zhou, Y., McMaster, M.T., and Fisher, S.J. (2000). Upregulation of human cytotrophoblast invasion by hepatocyte growth factor. J. Reprod. Fertil. Suppl. 55, 73–80.

Natale, D.R.C., Starovic, M., and Cross, J.C. (2006). Phenotypic analysis of the mouse placenta. Methods Mol. Med. 121, 275–293.

Plum, A., Winterhager, E., Pesch, J., Lautermann, J., Hallas, G., Rosentreter, B., Traub, O., Herberhold, C., and Willecke, K. (2001). Connexin31-deficiency in mice causes transient placental dysmorphogenesis but does not impair hearing and skin differentiation. Dev. Biol. 231, 334–347.

Rhodes, K.E., Gekas, C., Wang, Y., Lux, C.T., Francis, C.S., Chan, D.N., Conway, S., Orkin, S.H., Yoder, M.C., and Mikkola, H.K.A. (2008). The emergence of hematopoietic stem cells is initiated in the placental vasculature in the absence of circulation. Cell Stem Cell 2, 252–263.

Rinkevich, Y., Lindau, P., Ueno, H., Longaker, M.T., and Weissman, I.L. (2011). Germ-layer and lineage-restricted stem/progenitors regenerate the mouse digit tip. Nature 476, 409–413.

Rossant, J., and Cross, J.C. (2001). Placental development: lessons from mouse mutants. Nat. Rev. Genet. 2, 538–548.

Saito, S., Sakakura, S., Enomoto, M., Ichijo, M., Matsumoto, K., and Nakamura, T. (1995). Hepatocyte growth factor promotes the growth of cytotrophoblasts by the paracrine mechanism. J. Biochem. 117, 671–676.

Schmidt, C., Bladt, F., Goedecke, S., Brinkmann, V., Zschiesche, W., Sharpe, M., Gherardi, E., and Birchmeier, C. (1995). Scatter factor/hepatocyte growth factor is essential for liver development. Nature 373, 699–702.

Scifres, C.M., and Nelson, D.M. (2009). Intrauterine growth restriction, human placental development and trophoblast cell death. J. Physiol. 587, 3453–3458.

Simmons, D.G., and Cross, J.C. (2005). Determinants of trophoblast lineage and cell subtype specification in the mouse placenta. Dev. Biol. 284, 12–24.

Simmons, D.G., Natale, D.R.C., Begay, V., Hughes, M., Leutz, A., and Cross, J.C. (2008). Early patterning of the chorion leads to the trilaminar trophoblast cell structure in the placental labyrinth. Development 135, 2083–2091.

Sivasubramaniyam, T., Garcia, J., Tagliaferro, A., Melland-Smith, M., Chauvin, S., Post, M., Todros, T., and Caniggia, I. (2013). Where polarity meets fusion: role of Par6 in trophoblast differentiation during placental development and preeclampsia. Endocrinology 154, 1296–1309.

Somerset, D.A., Li, X.F., Afford, S., Strain, A.J., Ahmed, A., Sangha, R.K., Whittle, M.J., and Kilby, M.D. (1998). Ontogeny of hepatocyte growth factor (HGF) and its receptor (c-met) in human placenta: reduced HGF expression in intrauterine growth restriction. Am. J. Pathol. 153, 1139–1147.

Stecca, B., Nait-Oumesmar, B., Kelley, K.A., Voss, A.K., Thomas, T., and Lazzarini, R.A. (2002). Gcm1 expression defines three stages of chorio-allantoic interaction during placental development. Mech. Dev. 115, 27–34.

Takayanagi, T., Aoki, Y., and Tanaka, K. (2000). Expression of constitutively active c-MET receptor in human choriocarcinoma. Gynecol. Obstet. Invest. 50, 198–202.

Tanaka, S., Kunath, T., Hadjantonakis, A.K., Nagy, A., and Rossant, J. (1998). Promotion of trophoblast stem cell proliferation by FGF4. Science 282, 2072–2075.

Uehara, Y., Minowa, O., Mori, C., Shiota, K., Kuno, J., Noda, T., and Kitamura, N. (1995). Placental defect and embryonic lethality in mice lacking hepatocyte growth factor/scatter factor. Nature 373, 702–705.

Unezaki, S., Horai, R., Sudo, K., Iwakura, Y., and Ito, S. (2007). Ovol2/Movo, a homologue of Drosophila ovo, is required for angiogenesis, heart formation and placental development in mice. Genes Cells 12, 773–785.

Uy, G.D., Downs, K.M., and Gardner, R.L. (2002). Inhibition of trophoblast stem cell potential in chorionic ectoderm coincides with occlusion of the ectoplacental cavity in the mouse. Development 129, 3913–3924.

Van Handel, B., Prashad, S.L., Hassanzadeh-Kiabi, N., Huang, A., Magnusson, M., Atanassova, B., Chen, A., Hamalainen, E.I., and Mikkola, H.K. (2010). The first trimester human placenta is a site for terminal maturation of primitive erythroid cells. Blood 116, 3321–3330.

Watson, E.D., and Cross, J.C. (2005). Development of structures and transport functions in the mouse placenta. Physiology (Bethesda) 20, 180–193.

Wynne, F., Ball, M., McLellan, A.S., Dockery, P., Zimmermann, W., and Moore, T. (2006). Mouse pregnancy-specific glycoproteins: tissue-specific expression and evidence of association with maternal vasculature. Reproduction 131, 721–732.

Young, B.C., Levine, R.J., and Karumanchi, S.A. (2010). Pathogenesis of preeclampsia. Annu. Rev. Pathol. 5, 173–192.